J. Biochem. 121, 568-577 (1997)

Interaction with D-Glucose and Thermal Denaturation of Yeast Hexokinase B: A DSC Study[1]

F. Catanzano,* A. Gambuti,* G. Graziano,† and G. Barone*,[2]

*Dipartimento di Chimica, Università di Napoli "Federico II" Via Mezzocannone, 4-80134 Napoli, Italy; and †Dipartimento di Chimica, Università di Salerno Via Salvador Allende-84081 Baronissi (SA), Italy

Received for publication, October 28, 1996

DSC measurements have been performed on the monomeric form of yeast hexokinase B in the absence and presence of increasing concentrations of D-glucose. The hexokinase, in the absence of D-glucose, at both pH 8.0 and 8.5, shows reproducible calorimetric profiles characterized by the presence of two partially overlapped peaks. These can be ascribed to the presence of two structural domains in the native conformation of the enzyme, that possess different thermal stabilities and are denatured more or less independently. In the presence of saturating and increasing concentrations of D-glucose, the shape of the DSC profiles dramatically changes, since a single well-shaped peak is present. The binding of D-glucose enhances the interaction between the two lobes, as evidenced by the shrinking of the protein in overall dimensions, and gives rise to DSC profiles resembling those of a single domain protein. To deconvolve the DSC curves we considered a denaturation model consisting of two sequential steps with three macroscopic states of the protein and the binding of D-glucose only to the native state. We carried out two-dimensional nonlinear regression of the excess heat capacity surface constructed with the experimental DSC curves. This approach allows the calculation of a unique set of thermodynamic parameters characterizing both the thermal denaturation of hexokinase, and the binding equilibrium between D-glucose and the enzyme. It was found that the association constant is 9,800± 1,500 M^{-1} at pH 8.0. The binding of D-glucose is entropy-driven, since the binding enthalpy is zero. This finding is rationalized by a thermodynamic cycle for the association of two molecules in aqueous solution.

Key words: differential scanning calorimetry, thermodynamic stability, protein/ligand interaction.

The quantitative understanding of the noncovalent interactions that ensure the specificity and efficiency of binding processes is a fundamental step for clarifying a lot of relevant biological processes. For instance, proteins and enzymes that bind to carbohydrates are present in the majority of living organisms and are involved in a great variety of biological functions (*1*). Additionally, there is increasing interest in protein-carbohydrate interactions due to their essential role in biological recognition and adhesion processes. Differential scanning calorimetry, DSC, is an emerging technique for studying protein-ligand, protein-protein, and protein-nucleic acid interactions (*2-6*). Evaluation of thermodynamic binding parameters involves the observation of denaturation temperature changes and calorimetric profile alterations induced by association. Suitable thermodynamic models are needed to analyze the experimental data and to obtain quantitative results, as already demonstrated in an insightful paper by Brandts and Lin (*3*).

In continuous efforts to shed light on the thermodynamics of association phenomena (*7-9*), we considered it interesting to examine the interaction between hexokinase B and its specific ligand, D-glucose. According to the results of X-ray crystallography, the monomeric form of hexokinase B is composed of two lobes separated by a deep cleft in which the substrate is bound (*10, 11*). Upon binding of D-glucose, hexokinase B undergoes a large conformational change, both in the crystalline state and in aqueous solution (*12, 13*), which is considered as strong validation of the "induced-fit" mechanism proposed by Koshland (*14*). However, the major structural features of each lobe are preserved on the conformational change, justifying the characterization of the process as a rigid-body rotation. In fact, one lobe is rotated by 12° relative to the other, resulting in movements of as much as 9 Å in the polypeptide backbone and closure of the cleft. During this change, the accessible surface area of hexokinase is reduced, decreasing the exposure of both polar and nonpolar groups to the solvent (*12*).

We performed DSC measurements at pH 8.0 and 8.5 to characterize the unfolding process of hexokinase B in the absence and presence of D-glucose that, in addition to stabilization of the enzyme, causes a considerable change in the shape of calorimetric curves. Careful analysis of the

[1] This work was supported by grants from the Italian National Research Council (C.N.R., Rome), and the Ministry for University and Scientific and Technological Research (M.U.R.S.T., Rome), Programs "40%" of National Interest.

[2] To whom correspondence should be addressed. Fax: +39-81-5527771, E-mail: barone@chemna.dichi.unina.it

experimental data was carried out by constructing a two-dimensional excess heat capacity surface as a function of the temperature and ligand concentration (*15, 16*). Global linkage analysis, by means of a nonlinear regression procedure with respect to a proposed unfolding model, allowed us to calculate a unique set of thermodynamic parameters associated with both the temperature-induced denaturation of hexokinase B and the binding equilibrium of D-glucose. The reliability of the calculated binding parameters was confirmed by their agreement with values in the literature (*17*). Finally, a thermodynamic cycle, describing the association of two molecules in solution, is discussed to clarify the entropic driving force of D-glucose binding to hexokinase B.

MATERIALS AND METHODS

The yeast hexokinase used in this work was the B isoenzyme fraction II of the Kaji *et al.* preparation (*18*), purchased from Sigma as an ammonium sulphate precipitate and used without further purification. The commercial product is lacking 11 residues from the amino terminus due to proteolytic cleavage by an endogenous yeast protease (*19*). The proteolyzed enzyme is monomeric (M.W. 50 kDa) at basic pH and/or NaCl concentrations above 0.1 M (*17, 20, 21*). Polyacrylamide gel electrophoresis of the commercial product, under both native and denaturing conditions, was consistent with the enzyme being 95% pure and lacking the amino terminal fragment. D-Glucose was of analytical grade and obtained from Serva. The buffer employed was heppso (*N*-2-hydroxyethylpiperazine-*N'*-2-hydroxypropanesulfonic acid), 50 mM, pH 8.0 and 8.5, purchased from Sigma. It was preferable to the widely used Tris-HCl buffer due to its lower ionization enthalpy (*22*). Indeed, the ionization enthalpy of heppso is 30 kJ·mol^{-1} and $\Delta pK_a/^\circ C = -0.016$, while that of Tris is 48 kJ·mol^{-1} and $\Delta pK_a/^\circ C = -0.031$. pH measurements were performed at 25°C with a Radiometer pHmeter model PHM 93. Doubly deionized water was used throughout.

Enzyme solutions were exhaustively dialyzed at 4°C, using Spectra-Por MW 15,000 membranes, against 50 mM heppso buffer at pH 8.0 and 8.5. The hexokinase B concentrations in solutions were determined by absorbance measurements, using a specific absorptivity value of 0.947 cm^2·mg^{-1} (*17*). Sugars solutions were prepared by dissolving a weighed amount of material after drying for about 2 h *in vacuo* over P_2O_5. As a general rule, protein solutions must be employed within a few days because degradation can occur, resulting in non-reproducible measurements.

Scanning Calorimetry—Calorimetric measurements were carried out with a Setaram Micro-DSC apparatus. The instrument was interfaced with a data translation A/D board for automatic data acquisition. A scan rate of 0.5°C·min^{-1} was chosen for the present study. All data analyses were accomplished using software developed in our laboratory (*23, 24*). The calibration was performed exploiting the Joule effect by means of a specific Setaram apparatus. An electrical signal was applied for a time, t, and the instrument output was recorded. The integration of the obtained curve represents a quantity, A (μV·s). This value is then divided by the product of the power, P, used and the time t, giving a coefficient, $K = A/P\ t$, in μV/mW. The calibration was performed at different temperatures for a fixed scan rate. The experimental values were interpolated, generating a calibration curve in the range of 0–99°C. The raw data were converted to an apparent molar heat capacity by correcting for the instrument's calibration curve and the buffer-buffer scanning curve, and by dividing each data point by the scan rate and the protein molar concentration in the sample cell. Finally, the excess molar heat capacity function values, $\langle \Delta C_p \rangle$, were obtained after baseline subtraction, using the heat capacity of the native state as a reference (*25, 26*). Due to the low denaturation temperature of hexokinase *B*, and to avoid the problems in the analysis of experimental curves pointed out by Haynie and Freire (*27*), for reliable evaluation of the baseline the DSC scans were always started from 0°C.

The van't Hoff enthalpy was calculated with the commonly used formula (*28*):

$$\Delta_d H_{v.H} = 4\ RT_{max}^2 \cdot \langle \Delta C_p \rangle_{max} / \Delta_d H \qquad (1)$$

where $\langle \Delta C_p \rangle_{max}$ is the maximum height of the observable excess molar heat capacity, T_{max} is the temperature corresponding to $\langle \Delta C_p \rangle_{max}$, $\Delta_d H$ is the denaturation enthalpy change calculated by direct integration of the calorimetric peak, and R is the gas constant. Close correspondence between the calorimetric enthalpy, $\Delta_d H$, and the van't Hoff enthalpy, $\Delta_d H_{v.H.}$, is a necessary condition to state that the denaturation is a two-state transition (*25, 28*).

Thermodynamic Model—Following the suggestion of Gill and co-workers (*29*), we developed a sequential thermodynamic model that considers the presence of an intermediate state between the native and denatured ones, and the binding of a specific ligand to one site of the native conformation. The overall process is described by the following scheme:

$$\begin{array}{ccccc} & & K_1 & & K_2 & \\ & N & \leftrightarrow & I & \leftrightarrow & D \\ K_b[L] & \uparrow & & \uparrow & & K'[L] \\ & & \rightarrow NL \leftarrow & & & \end{array}$$

where N is the native state, I the intermediate, D the denatured state, and NL the native state with the binding site filled by the ligand. K_1 is the equilibrium constant of the conformational transition, N↔I and is temperature-dependent according to:

$$K_1 = \exp - \{ [\Delta_N{}^I H(T_{d,1})/R](1/T - 1/T_{d,1}) + (\Delta_N{}^I C_p/R)[1 - (T_{d,1}/T) + \ln(T/T_{d,1})] \} \qquad (2)$$

where $T_{d,1}$ is the denaturation temperature when $K_1 = 1$, $\Delta_N{}^I H(T_{d,1})$ is the enthalpy change associated with the transition, N↔I, and $\Delta_N{}^I C_p$ is the corresponding heat capacity change. Similarly, K_2 is the equilibrium constant of the conformational transition, I↔D, and is temperature-dependent according to:

$$K_2 = \exp - \{ [\Delta_I{}^D H(T_{d,2})/R](1/T - 1/T_{d,2}) + (\Delta_I{}^D C_p/R)[1 - (T_{d,2}/T) + \ln(T/T_{d,2})] \} \qquad (3)$$

where $T_{d,2}$ is the denaturation temperature when $K_2 = 1$, $\Delta_I{}^D H(T_{d,2})$ is the enthalpy change associated with the transition, I↔D, and $\Delta_I{}^D C_p$ is the corresponding heat capacity change. Clearly Eqs. 2 and 3 are exact with the assumption that the heat capacity changes are temperature-independent. Finally, K_b is the equilibrium binding constant and depends on temperature according to:

$$K_b = K_b^* \exp - [(\Delta_b H/R)(1/T - 1/298.15)] \qquad (4)$$

where K_b° is the value of K_b at 298.15 K and $\Delta_b H$ is the enthalpy change associated with the binding equilibrium, which is considered to be temperature-independent. It was readily verified that K', the equilibrium constant of the process, NL↔I+L, is equal to K_1/K_b, and so K_1, K_2, and K_b are the only independent parameters necessary to fully characterize the proposed model. The macroscopic canonical partition function (*25, 29*) is given by:

$$\begin{aligned} Q(T) &= [N] + [NL] + [I] + [D] \\ &= [N](1 + K_b[L] + K_1 + K_1K_2) \end{aligned} \quad (5)$$

Taking the native state as a reference, it becomes:

$$Q_N(T) = 1 + K_b[L] + K_1 + K_1K_2 \quad (6)$$

The excess enthalpy function, with respect to the native state, can be readily obtained with the general statistical mechanical relationship:

$$\langle \Delta H(T) \rangle = RT^2(\partial \ln Q_N/\partial T)_{P,[L]} \quad (7)$$

that gives:

$$\begin{aligned} \langle \Delta H \rangle = {} & \\ & [\Delta_N{}^I H(T_{d,1}) + \Delta_N{}^I C_p(T - T_{d,1})](K_1/Q_N) \\ & + [\Delta_N{}^I H(T_{d,1}) + \Delta_N{}^I C_p(T - T_{d,1}) + \Delta_I{}^D H(T_{d,2}) \\ & + \Delta_I{}^D C_p(T - T_{d,2})](K_1K_2/Q_N) + \Delta_b H(K_b[L]/Q_N) \end{aligned} \quad (8)$$

When the total ligand concentration is much greater than the protein concentration, as under our experimental conditions, the free ligand concentration [L] can be considered to be constant with increasing temperature in a DSC scan. Therefore, the excess heat capacity function, which is physically observable on DSC measurements, is given by:

$$\langle \Delta C_p(T) \rangle = (\partial \langle \Delta H \rangle / \partial T)_{P,[L]} \quad (9)$$

This model is able to simulate DSC curves by using as input parameters the values of $T_{d,1}$, $\Delta_N{}^I H(T_{d,1})$, $\Delta_N{}^I C_p$, $T_{d,2}$, $\Delta_I{}^D H(T_{d,2})$, $\Delta_I{}^D C_p$, K_b°, $\Delta_b H$ and [L]. When [L] can be considered equal to the total ligand concentration in solution, as in our case, the number of parameters necessary to describe an experimental DSC curve would be 8. This is also the number of parameters to be determined by the deconvolution procedure. To reduce the number of independent parameters, we eliminated the total heat capacity change associated with the temperature-induced transition (namely $\Delta_d C_p = \Delta_N{}^I C_p + \Delta_I{}^D C_p$), using an iterative procedure. Bearing in mind that the sigmoidal baseline is proportional to the progress of the unfolding reaction, as measured as the uptake of enthalpy at temperature T, $\Delta_d C_p$ is subtracted from the function, $\langle \Delta C_p(T) \rangle$, distributing it over the whole denaturation range (*30, 31*). The weighting of each point is determined by the ratio of the incremental area to the total area, and by iterating the process until convergence. In the first step of iteration the total area is calculated using a straight line connecting the initial and final points of a peak. Adopting this approach, the number of parameters necessary to calculate a DSC curve is 6 [namely, $T_{d,1}$, $\Delta_N{}^I H(T_{d,1})$, $T_{d,2}$, $\Delta_I{}^D H(T_{d,2})$, K_b° and $\Delta_b H$]. We developed a program that allows deconvolution of an experimental curve with respect to Eq. 9, using the Levenberg-Marquardt algorithm (*32*), as implemented in the Optimization Toolbox of MATLAB®.

However, for more reliable evaluation of thermodynamic parameters from a statistical point of view, we followed the procedure devised by Freire and Straume (*15, 16*), and constructed an experimental excess heat capacity surface as a function of the temperature and ligand concentration. Nonlinear regression of the entire surface with respect to Eq. 9 was carried out until a convergence criterion was satisfied (*16*). Nonlinear, joint confidence intervals were determined for all estimated parameters according to the method developed by Johnson and Frasier (*33, 34*). Such two-dimensional analysis of the excess heat capacity allows the evaluation of a unique best set of thermodynamic parameters characterizing both the thermal denaturation of a globular protein, and the binding equilibrium between a ligand and a macromolecule. Finally, it must be noted that, as $\Delta_d C_p$ was eliminated from the excess heat capacity profiles, the values of $\Delta_N{}^I C_p$ and $\Delta_I{}^D C_p$ for individual transitions cannot be evaluated by normal deconvolution. However, two-dimensional deconvolution allows one to estimate $\Delta_N{}^I C_p$ and $\Delta_I{}^D C_p$, because these parameters partially determine the area and, to a lesser extent, the location of DSC peaks with changing ligand concentration.

RESULTS

We performed DSC measurements on the monomeric form of yeast hexokinase B in the absence and presence of increasing concentrations of D-glucose. As already reported (*17, 20, 21, 35*), the monomeric form of hexokinase B is only stable under suitable experimental conditions. Even though the commercial product is lacking 11 residues from the N-terminal end, a condition that strongly favors the monomeric form, it was necessary to carry out the measurements at alkaline pHs (namely pH 8.0 and 8.5 in 50 mM heppso buffer) to avoid the presence in solution of the dimeric form (*19*). Additionally, even the protein concentration, in the absence of D-glucose, is a significant variable. The experimental DSC measurements were performed in the concentration range of 1.2–2.5 mg·ml^{-1}. It is not possible to use concentrations below 1.2 mg·ml^{-1} due to the sensitivity limits of the DSC instrument. On the other hand, to be sure that only the monomeric form of hexokinase B is present in solution, it is not possible to employ concentrations above 3.0 mg·ml^{-1}. A greater concentration of hexokinase B, in the absence of D-glucose in the solution, shifts the monomer to dimer equilibrium toward the formation of substantial amounts of the dimeric form (*19*). The calorimetric profile of hexokinase B at $c = 4.9$ mg·ml^{-1} and pH 8.0 in 50 mM heppso buffer is shown in Fig. 1. The thermogram is very complex, because there are three peaks, the first two being partially overlapped and the third smaller, occurring at a higher temperature, about 58°C. We have not further investigated the origin of the last peak; likely, it can be ascribed to the thermal denaturation of the dimeric form, since oligomerization seems to be a general strategy for protein stabilization (*36*).

In the concentration range employed (1.2–2.5 mg·ml^{-1}), the hexokinase B, in the absence of D-glucose, at both pH 8.0 and 8.5, shows reproducible calorimetric profiles characterized by the presence of two partially overlapped peaks (see Fig. 2, curves a and b). They can be ascribed to the presence of two structural domains in the native conformation of monomeric hexokinase B, that possess different thermal stabilities and are denatured more or less independently. The existence of two structural domains in yeast hexokinase was firmly established by the X-ray three-

dimensional structure of this enzyme (*10, 11*). There is no evidence of additional humps at high temperature in the DSC traces; this is a strong indication that under these experimental conditions only the monomeric form of hexokinase B exists. The thermodynamic parameters obtained directly on the analysis of DSC curves are presented in Table I. On moving from pH 8.0 to 8.5 the temperature corresponding to the maximum of the DSC curve increases from 46.7°C to 48.2°C, and the calorimetric enthalpy increases from 700 to 750 kJ·mol^{-1}. Clearly the process does not correspond to a two-state transition, as confirmed by the non-coincidence of the van't Hoff enthalpy with the calorimetric one. On the other hand, the denaturation heat capacity change is not affected by the change in pH, the average value being $\Delta_d C_p = 30.0$ kJ·K^{-1}·mol^{-1}. This value is in agreement with that calculated with a model developed by some of us, and based on average structural features of globular proteins, and the specific contributions to the heat capacity change of polar and nonpolar groups (*37, 38*). For monomeric hexokinase B, of 461 residues and 50 kDa, the calculated $\Delta_d C_p = 35.0$ kJ·K^{-1}·mol^{-1}. It must be stressed that the temperature-induced denaturation of hexokinase B is an irreversible process according to the reheating criterion (this aspect will be discussed later).

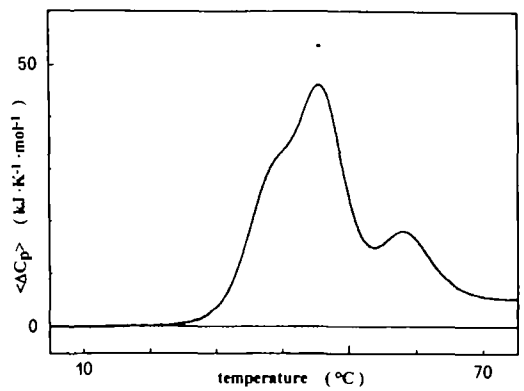

Fig. 1. **Experimental DSC profile of yeast hexokinase B at pH 8.0, in 50 mM heppso buffer, with a protein concentration of 4.9 mg·ml^{-1}.** The small third peak at high temperature is probably due to the presence of a substantial amount of the dimeric form of the enzyme.

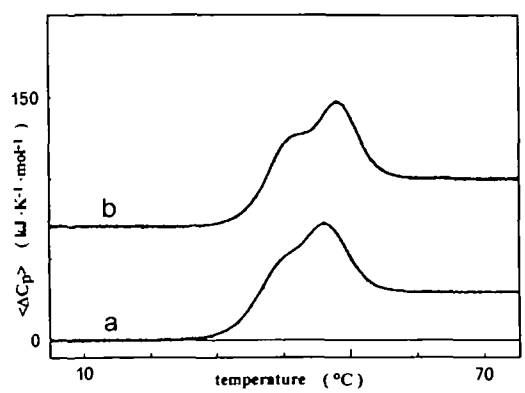

Fig. 2. **Experimental DSC profiles of yeast hexokinase B at pH 8.0 (c=1.25 mg·ml^{-1}, curve a), and pH 8.5 (c=2.45 mg·ml^{-1}, curve b), in 50 mM heppso buffer.** Excess heat capacity values have been shifted along the y-axis for ease of presentation.

DSC measurements were performed in the presence of saturating and increasing concentrations of D-glucose: up to 1.5 M at pH 8.0 and up to 80 mM at pH 8.5, the concentration of hexokinase B being fixed at 1.75 mg·ml^{-1}, in order to reduce the number of independent variables. In an aqueous solution D-glucose forms an equilibrium mixture of the α and β anomeric forms: 37% of α form at 25°C and ΔH ($\alpha \rightarrow \beta$) = −1.16 kJ·mol^{-1} (*39*). However, hexokinase, like other enzymes of glucose metabolism (*e.g.*, glucokinase and glucose-6-phosphatase), is able to act on both anomeric forms of D-glucose (*1*). Therefore the mutarotation equilibrium does not affect the results. The thermodynamic parameters derived from the experimental curves are presented in Table II. Even under these conditions the process is irreversible, but the shape of the DSC profile dramatically changes since a single well-shaped peak is present. The binding of D-glucose enhances the interaction between the two lobes, as evidenced by the shrinking of the protein in overall dimensions (*12, 13*), and gives rise to DSC profiles resembling those of a single domain protein, even though the van't Hoff enthalpy values are always lower than the calorimetric ones. Additionally, the temperature of the maximum of the DSC peak increases with increasing D-glucose concentration. At pH 8.0, the denatur-

TABLE I. **Thermodynamic parameters of the thermal denaturation of hexokinase B at pH 8.0 and 8.5, in 50 mM heppso buffer.** The values of $\Delta_d H_{v\,H}$ were calculated according to Eq. 1.

pH	Hexokinase (mg·ml^{-1})	T_{max} (°C)	$\Delta_d H$ (kJ·mol^{-1})	$\Delta_d H_{v,H}$ (kJ·mol^{-1})	$\Delta_d C_p$ (kJ·K^{-1}·mol^{-1})
8.0	1.25	46.6	690	360	29
	1.75	46.7	700	340	30
	2.50	46.7	700	360	30
8.5	1.30	48.1	745	410	31
	1.75	48.2	750	400	30
	2.45	48.2	750	415	29

Note: Each figure represents the average value for three or four measurements. The error in T_{max} does not exceed 0.2°C. The estimated (relative) uncertainties in $\Delta_d H$ and $\Delta_d C_p$ amount to 5 and 10%, respectively, of the reported values.

TABLE II. **Thermodynamic parameters of the thermal denaturation of hexokinase B (c=1.75 mg·ml^{-1}), at pH 8.0 and 8.5, in the presence of saturating and increasing D-glucose concentrations.** The values of $\Delta_d H_{v\,H}$ were calculated according to Eq. 1.

pH	D-Glucose (mM)	T_{max} (°C)	$\Delta_d H$ (kJ·mol^{-1})	$\Delta_d H_{v,H}$ (kJ·mol^{-1})	$\Delta_d C_p$ (kJ·K^{-1}·mol^{-1})
8.0	0	46.7	700	340	30.0
	10	48.4	750	610	32.0
	30	49.4	780	640	29.0
	50	50.0	800	700	31.0
	80	50.5	820	700	28.0
	100	52.0	870	740	30.0
	300	54.0	930	790	33.0
	500	56.0	1,000	890	29.0
	800	58.0	1,060	960	30.0
	1,000	59.7	1,120	1,030	33.0
	1,500	62.2	1,200	1,090	35.0
8.5	0	48.2	750	400	30.0
	10	49.5	790	580	30.0
	30	50.4	820	670	31.0
	80	51.7	860	730	32.0

Note: Each figure represents the average value for three or four measurements. The error in T_{max} does not exceed 0.2°C. The estimated (relative) uncertainties in $\Delta_d H$ and $\Delta_d C_p$ amount to 5 and 10%, respectively, of the reported values.

ation temperature increases from 46.7°C for the hexokinase alone to 62.2°C with 1.5 M D-glucose. In the same way, the denaturation enthalpy rises from 700 kJ·mol^{-1} for the hexokinase alone to 1,200 kJ·mol^{-1} with 1.5 M D-glucose. This increase is caused by the large positive heat capacity change associated with the denaturation, that is not significantly affected by the presence of D-glucose in the solution, at least for the concentration range investigated in this study. In this regard, it is interesting to note the strong dependence of $\Delta_d C_p$ on the composition of the solution brought out for RNase A and lysozyme (*40*). Very similar results were obtained at pH 8.5, where the denaturation temperature and enthalpy increased from 48.2°C and 750 kJ·mol^{-1} for the hexokinase alone to 51.7°C and 860 kJ·mol^{-1} with 80 mM D-glucose.

The irreversibility of the temperature-induced denaturation would strictly prevent more detailed analysis of DSC curves, as it is based on equilibrium thermodynamics. However, we observed that the shapes of DSC peaks and their locations along the temperature axis are not affected by the scanning rate in the range of 0.2-1.0°C min^{-1}. Additionally, after heating the protein up to the temperature corresponding to the maximum of the DSC peak and then cooling down to 0°C, a second scan of the same sample shows high recovery of the endothermic peak. Both these findings seem to suggest that the process is not kinetically controlled. Likely, the purely conformational transition is reversible, and the irreversibility is due to side-reactions, occurring at alkaline pH and high temperature, that prevent the correct refolding of the polypeptide chain on cooling of the solution (*41, 42*). In fact, Sturtevant and co-workers (*17*) reported: "It appears that the thermal unfolding of hexokinase, which may be reversible, is accompanied by considerable irreversible denaturation under the conditions of the DSC experiments." For these reasons we believed it reliable to apply equilibrium thermodynamics to deconvolve the DSC curves, as already performed by several authors in similar cases (*43-47*).

We considered a denaturation model consisting of two sequential steps with three macroscopic states of the protein and the binding of D-glucose only to the native state. This model can be used to analyze DSC profiles in the absence and presence of D-glucose in the solution. First, we carried out nonlinear regression of the DSC curves for the protein alone, and the results are presented in the second columns of Tables III and IV. Second, we performed two-dimensional nonlinear regression of an excess heat capacity surface constructed with the experimental DSC curves, after subtraction of the total denaturation heat capacity change. Two-dimensional deconvolution was only performed on the DSC curves in the range of 0-80 mM D-glucose, at both pH 8.0 and 8.5. When the D-glucose concentration is 100 mM and higher, its aspecific stabilizing action toward globular proteins largely overwhelms the effects due to its specific binding in the cleft of hexokinase B and the subsequent conformational change. This is emphasized by the continuous and marked increase in the denaturation temperature with increasing D-glucose concentration, that cannot be reproduced with the proposed model, unless the binding constant value is considerably raised. Therefore, the developed model can be applied only for D-glucose concentrations low enough to render the aspecific stabilization a negligible effect (*48, 49*).

The results are presented in the third columns of Tables III and IV. The calculated profiles are the continuous lines superimposed on the experimental traces in Figs. 3 and 4. It is evident that the overall agreement between the experimental and calculated curves is satisfactory. It should be stressed that, in the presence of saturating concentrations of D-glucose, the model gives rice automatically to a single peak, exactly as occurs in the experiments. Furthermore, the closeness of the thermodynamic parameters obtained on the deconvoluiton of DSC curves for hexokinase B in the absence and presence of D-glucose constitutes firm validation of the reliability of the performed thermodynamic analysis. The values of $\Delta_N{}^I H(T_{d,1})$, 310±30 kJ·mol^{-1} at pH 8.0 and 360±35 kJ·mol^{-1} at pH 8.5, representing the enthalpy change associated with the transition, N↔I, correspond roughly to half the total area of the endothermic peak. Also, the value of $\Delta_N{}^I C_p = 13$ kJ·K^{-1}·mol^{-1} is nearly half the total denaturation heat capacity change. These findings strongly suggest that the intermediate state has one lobe unfolded and the other intact. It is worth noting that the sum of the values of $\Delta_N{}^I C_p$ and $\Delta_I{}^D C_p$, obtained on the two-dimensional deconvolution, is close to the value of the total heat capacity change, obtained directly on DSC measurements, *i.e.*, 28 kJ·K^{-1}·mol^{-1} against 30 kJ·K^{-1}·mol^{-1}. The binding constant of D-glucose is about 9,500 M^{-1} at both pHs, while the binding enthalpy is zero. Therefore, the binding of D-glucose is

TABLE III. **Thermodynamic parameters obtained on deconvolution analysis of the experimental DSC curves of hexokinase B at pH 8.0 in the absence and presence of D-glucose, according to the sequential and independent transition models.** The two-dimensional deconvolution was performed on the DSC curves in the range of 0-80 mM D-glucose.

pH 8.0	Hexokinase (Seq.)	Hexokinase+ glucose (Seq.)	Hexokinase (Ind.)
$T_{d,1}$(°C)	38.8±0.5	38.9±0.6	38.7±0.4
$\Delta_N{}^I H$ ($T_{d,1}$) (kJ·mol^{-1})	320±20	310±30	325±20
$\Delta_N{}^I C_p$ (kJ·K^{-1}·mol^{-1})	–	13±2	–
$T_{d,2}$(°C)	46.6±0.5	46.9±0.6	46.7±0.5
$\Delta_I{}^D H$ ($T_{d,2}$) (kJ·mol^{-1})	380±25	380±25	390±30
$\Delta_I{}^D C_p$ (kJ·K^{-1}·mol^{-1})	–	15±3	–
K_b* (M^{-1})	–	9,800±1500	–
$\Delta_b H$ (J·mol^{-1})	–	0±200	–
σ (J·K^{-1}·mol^{-1})	530	3,920	610

Note: σ is the standard deviation of the fit.

TABLE IV. **Thermodynamic parameters obtained on deconvolution analysis of the experimental DSC curves of hexokinase B at pH 8.5 in the absence and presence of D-glucose, according to the sequential and independent transition models.** The two-dimensional deconvolution was performed on the DSC curves in the range of 0-80 mM D-glucose.

pH 8.5	Hexokinase (Seq.)	Hexokinase+ glucose (Seq.)	Hexokinase (Ind.)
$T_{d,1}$(°C)	40.2±0.5	40.6±0.4	40.4±0.5
$\Delta_N{}^I H(T_{d,1})$ (kJ·mol^{-1})	350±35	360±35	355±40
$\Delta_N{}^I C_p$ (kJ·K^{-1}·mol^{-1})	–	13±3	–
$T_{d,2}$ (°C)	48.2±0.5	48.7±0.4	48.6±0.5
$\Delta_I{}^D H$ ($T_{d,2}$) (kJ·mol^{-1})	400±30	400±25	405±30
$\Delta_I{}^D C_p$ (kJ·K^{-1}·mol^{-1})	–	15±3	–
K_b* (M^{-1})	–	9,500±1,600	–
$\Delta_b H$ (J·mol^{-1})	–	0±200	–
σ (J·K^{-1}·mol^{-1})	580	2,170	630

Note: σ is the standard deviation of the fit.

entropy-driven, being actually athermic.

It is also possible to consider that the monomeric form of hexokinase B is composed of two independent domains corresponding to the two lobes present in its three-dimensional structure. The independent domain transition model, assuming that each domain has two accessible conformations, *i.e.*, native and denatured ones, gives rise to four macroscopic states. They can be called NN* (completely folded conformation), ND* and DN* (partially unfolded conformations), and DD* (completely unfolded conformation), where N and D refer to one of the two cooperative domains, and N* and D* to the other. The denaturation process is described by the following scheme:

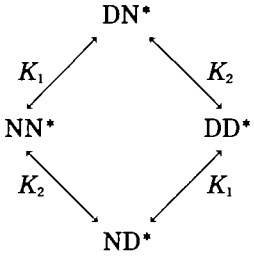

where K_1 is the equilibrium constant of the transition, NN* $\leftrightarrow$DN*, and K_2 is the equilibrium costant of the transition, NN* $\leftrightarrow$ND*. Clearly, if the two domains are independent, the two pairs of transitions are equal, as indicated in the scheme. The macroscopic canonical partition function, taking the completely folded conformation as the reference state, is:

$$Q(T)^{IND} = (1+K_1)\cdot(1+K_2) = 1+K_1+K_2+K_1K_2 \quad (10)$$

From this relationship, following the procedure shown under "MATERIALS AND METHODS," it is possible to derive an expression of the excess heat capacity function and to perform deconvolution of the experimental curves with respect to this scheme. As shown in the fourth columns of Tables III and IV (the symbols for the enthalpy and heat capacity changes are the same as those in the sequential model to simplify the notation), this model is able to fit well the DSC curves of hexokinase in the absence of D-glucose. The calculated thermodynamic parameters agree with those obtained with the sequential model. Looking at the schemes of the two models, it is possible to conclude that the results are very similar because only one of the two allowed ways to accomplish the unfolding process for the independent transition model is physically significant. In view of the domain structure of hexokinase B, one of the two domains is less stable and unfolds at lower temperatures than the other. Thus the denaturation process approaches a sequential mechanism. The connection between the two representations relies on the number of thermodynamic states which are significantly populated to contribute appreciably to the energetics of the denaturation process.

The use of the independent domain model may become ambiguous in the presence of a ligand, because it would be necessary to specify how the binding affects the properties of each of the two domains, *i.e.*, on which one the binding site is localized, or if the binding site is at the interface between the two domains (*47*). In the present case we have enough information to select among the different possibilities, even though this does not happen in general. An independent domain model in which only NN* binds to D-glucose is physically reliable. However, the application of such a model would give numerical results entirely consistent with those obtained with the sequential model, because we have shown that the thermal denaturation of hexokinase is well represented by a sequential mechanism. For this reason we did not attempt to use it to analyze the DSC curves of hexokinase B in the presence of D-glucose. On the other hand, the sequential model, since it does not consider the existence of structural domains in the protein, but treats the macromolecule as a unique object, allows unified analysis of the DSC measurements of hexokinase B in the absence and presence of D-glucose.

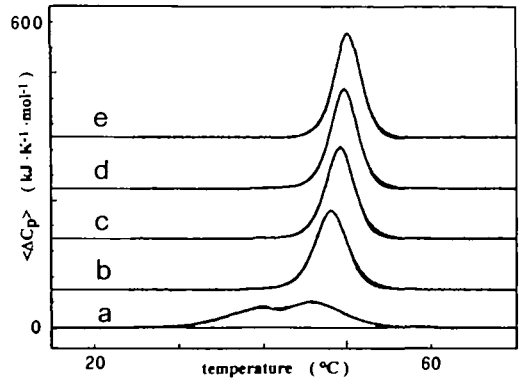

Fig. 3. **A set of DSC profiles of hexokinase B/D-glucose complexes at pH 8.0, with D-glucose concentrations of 0 (curve a), 10 mM (curve b), 30 mM (curve c), 50 mM (curve d), and 80 mM (curve e).** The hexokinase B concentration was fixed at 1.75 mg·ml^{-1}. The solid lines represent the best fit of the experimental curves calculated on two-dimensional nonlinear regression with respect to Eq. 9. See the text for more details. The curves have been shifted along the *y*-axis for clarity.

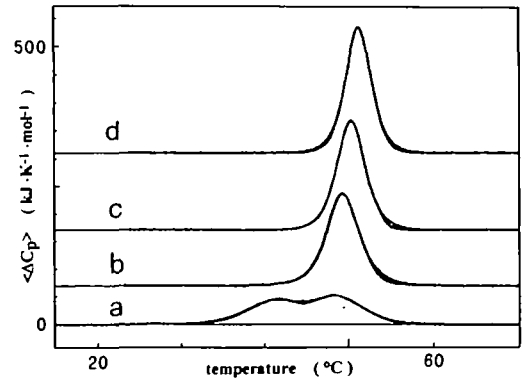

Fig. 4. **A set of DSC profiles of hexokinase B/D-glucose complexes at pH 8.5, with D-glucose concentrations of 0 (curve a), 10 mM (curve b), 30 mM (curve c), and 80 mM (curve d).** The hexokinase B concentration was fixed at 1.75 mg·ml^{-1}. The solid lines represent the best fit of the experimental curves calculated on two-dimensional nonlinear regression with respect to Eq. 9. See the text for more details. The curves have been shifted along the *y*-axis for clarity.

DISCUSSION

To our knowledge only one DSC study has been reported in the literature on the thermal denaturation of the monomeric form of yeast hexokinase B, in the absence and presence of D-glucose. Sturtevant and co-workers performed DSC measurements at pH 8.5 in Tris-HCl buffer and the process was irreversible (*17*). They found that the free enzyme gave a calorimetric profile with two maxima, centered at 41.0 and 48.0°C, at low ionic strength (5 mM Tris-HCl buffer), and with only one maximum, centered at 42.5°C, at high ionic strength (5 mM Tris-HCl buffer plus 200 mM NaCl). The DSC curve for the unfolding of the glucose-bound enzyme had only one peak, at both low and high ionic strength, centered around 51.0°C. They also found a substantial $\Delta_d C_p$ in the DSC curves of hexokinase B in the absence and presence of D-glucose at low ionic strength, but did not report any value. It is not possible to make a one to one comparison between our results and those of Sturtevant because the experimental conditions used were different. One point must be especially stressed. These researchers used Tris-HCl buffer for pH 8.5; but, in view of the large heat of ionization of Tris, it must be assumed that the pH decreased by almost 1 unit for the temperature interval, 25–60°C. Furthermore, we carried out a set of preliminary DSC measurements in Tris-HCl buffer at pH 8.5 (*50*), and the results were not very reproducible, as also found by others (*51*). In any case, our actual results with heppso buffer are in qualitative agreement with those of Sturtevant and co-workers at low ionic strength.

One of the principal merits of two-dimensional deconvolution of an excess heat capacity surface is the possibility of calculating reliable thermodynamic parameters characterizing the binding equilibrium (*9, 15*). As found on analysis of the system, D-glucose/hexokinase B, $K_b^* = 9{,}800 \pm 1{,}500\ M^{-1}$ at pH 8.0 and $9{,}500 \pm 1{,}600\ M^{-1}$ at pH 8.5, and $\Delta_b H = 0 \pm 200\ J \cdot mol^{-1}$ at both pHs. These binding constant estimates are in satisfactory agreement with values in the literature, bearing in mind the different experimental approaches employed. Indeed, DSC is an indirect technique for studying binding equilibria, and in our case the binding constant values may be partially affected by the aspecific stabilizing action of glucose, which shifts the denaturation temperature. Sturtevant and co-workers (*17*), by means of fluorescence titration, found that $K_b = 5{,}650 \pm 350\ M^{-1}$ at 25°C and pH 8.5 in 5 mM Tris-HCl buffer plus 200 mM NaCl. Kellet and colleagues (*52*) determined $K_b = 2{,}650 \pm 200\ M^{-1}$ at 25°C and pH 6.7, in 40 mM Tris-HCl buffer plus 1 mM citrate, performing fluorescence quenching measurements. Additionally, they found that $K_b = 3{,}350 \pm 250\ M^{-1}$ at 25°C and pH 8.5, in 50 mM Tris-HCl buffer, independent of the ionic strength, for the proteolytically modified hexokinase B (*53*).

The calculated binding enthalpy is practically zero and this finding also agrees with Sturtevant's work (*17*). Indeed the binding enthalpy was determined by isothermal flow and batch calorimetry in the temperature range, 7–29°C, at both low and high ionic strength, and by van't Hoff plotting of the equilibrium constants, obtained by fluorescence titration in the temperature range of 5–28°C at high ionic strength. The two independent determinations resulted unequivocally in a binding enthalpy of practically zero and in a heat capacity change also virtually zero. These results seem reliable. Nevertheless, it appears strange that the binding of D-glucose to hexokinase B, which leads to a large conformational rearrangement of the protein structure, is associated with a negligible heat effect. Likely, nearly perfect compensation of exothermic and endothermic subprocesses occurs, and the binding of D-glucose is entropically driven.

To clarify the molecular origin of the entropy gain responsible of the binding, we suggest for the molecular association of two bodies in water, the thermodynamic cycle schematically shown in Fig. 5, following recent theoretical approaches (*54-56*). According to this cycle the Gibbs energy change associated with the binding is given by:

$$\begin{aligned}\Delta G_b = {} & \Delta G_{c(w),AB} - \Delta G_{c(w),A} - \Delta G_{c(w),B} + \Delta G_{a(w),AB} + \Delta G_{a,AB} \\ & - \Delta G_{a(w),A} - \Delta G_{a(w),B} + \Delta G_{r(w),AB} - \Delta G_{r(w),A} \\ & - \Delta G_{r(w),B} + \Delta G_{r,AB} - T\,\Delta S_{tr,rot} \qquad (11)\end{aligned}$$

where $\Delta G_{c(w),AB}$, $\Delta G_{c(w),A}$, and $\Delta G_{c(w),B}$ are the Gibbs energy changes to create in water cavities to be occupied by complex AB, and molecules A and B. Lee showed that the Gibbs energy cost to create a cavity in a solvent is of a purely entropic nature, originating from an excluded volume effect (*57, 58*). $\Delta G_{a(w),AB}$, $\Delta G_{a(w),A}$, and $\Delta G_{a(w),B}$ are the interaction energies of AB, A, and B with the surrounding water molecules; $\Delta G_{a,AB}$ is the interaction energy of A and B in the complex. These four terms are considered purely energetic contributions (*54, 57*). $\Delta G_{r(w),AB}$, $\Delta G_{r(w),A}$, and $\Delta G_{r(w),B}$ are the Gibbs energy changes associated with water reorganization upon insertion of complex AB, and molecules A and B (*59*). Finally $\Delta G_{r,AB}$ represents the Gibbs energy change associated with induced-fit conformational changes in the complex, and $-T\Delta S_{tr,rot}$ corresponds to the loss of translational and rotational entropy on complex formation (*60*).

For the binding of D-glucose to hexokinase B, due to the very large difference in molecular dimensions, it is possible to assume, as a first approximation, that: $\Delta G_{c(w),AB} \cong \Delta G_{c(w),A}$, and $\Delta G_{a(w),AB} - \Delta G_{a(w),A} + \Delta G_{r(w),AB} - \Delta G_{r(w),A} \cong 0$, where A stands for the enzyme and B for the small ligand. Therefore it is:

$$\begin{aligned}\Delta G_b \cong {} & -\Delta G_{c(w),B} + \Delta G_{a,AB} - \Delta G_{a(w),B} - \Delta G_{r(w),B} \\ & + \Delta G_{r,AB} - T\Delta S_{tr,rot} \qquad (12)\end{aligned}$$

According to the X-ray structure of the complex (*10, 11*), D-glucose completely loses its first hydration shell when bound to hexokinase. The corresponding energy penalty is counterbalanced by the formation of seven new hydrogen bonds between the sugar and the residues lining the binding cleft, and by the energetic contributions arising from water reorganization upon solute removal and the structural relaxation of the formed complex. In other words, the term, $[-\Delta G_{a(w),B}]$, is nearly compensated for by the sum of $[+\Delta G_{a,AB}]$, and the energetic components of the procees of reorganization of water after removal of D-glucose $[-\Delta H_{r(w),B}]$, and of hexokinase as a consequence of the induced fit $[+\Delta H_{r,AB}]$. After cancellation of these energetic terms, Eq. 12 becomes:

$$\Delta G_b \cong -\Delta G_{c(w),B} + T\Delta S_{r(w),B} - T\Delta S_{r,AB} - T\Delta S_{tr,rot} \qquad (13)$$

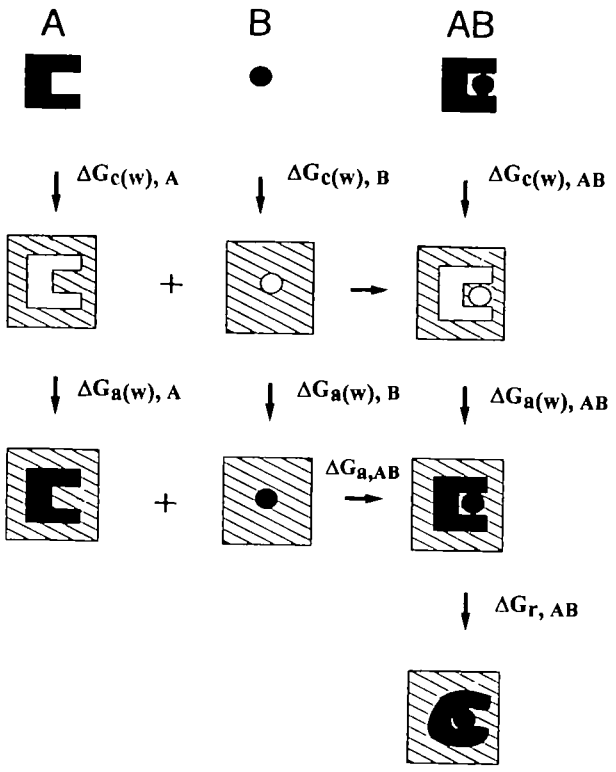

Fig. 5. **Thermodynamic cycle for the association of two molecules in a solvent in terms of cavitation Gibbs energy, solute-solvent and solute-solute interaction Gibbs energies, and Gibbs energy contributions due to solvent reorganization and complex structural relaxation.** See the text for more details.

The four terms on the right-hand side are purely entropic, and the larger contributions are likely given by the first, second and fourth terms. The first represents the gain in Gibbs energy associated with closure of the cavity occupied by D-glucose in water, the second represents the entropic gain due to the release of water molecules from the D-glucose hydration shell, and the fourth accounts for the loss of translational and rotational degrees of freedom on complex formation. The third term is the entropic contribution arising from the hexokinase conformational change upon binding, and is probably very small, since the process corresponds to a rigid body rotation. This analysis clarifies that the molecular origin of the entropy gain, driving the binding of D-glucose to hexokinase, is the gain in both the configurational space, and the translational and rotational degrees of freedom by water molecules after removal of the ligand from the solution upon complex formation.

The other important thermodynamic aspect of D-glucose binding to hexokinase B is the zero heat capacity change. This finding requires an explanation. In the present case two main sub-processes contribute to $\Delta_b C_p$: removal of D-glucose from water to form the complex and closure of the cleft. The heat capacity change associated with the dissolution of solid D-glucose in water is $128 \pm 3\ J \cdot K^{-1} \cdot mol^{-1}$ at 25°C (*61*), and the expected contribution to $\Delta_b C_p$ is extremely small. The closure of the cleft upon binding causes the burial of about 300 Å² of the accessible surface area, ASA (*12*), and the release of about 30 water molecules (*62*). The ASA buried, being involved in the recognition of a polar molecule, such as D-glucose, surely contains both polar and nonpolar groups. Their burial makes opposing and likely compensating contributions to $\Delta_b C_p$ (*63*). Thus this analysis is able to justify the experimental finding of a zero heat capacity change associated with the binding of D-glucose to hexokinase B.

CONCLUSION

We investigated the temperature-induced denaturation of hexokinase B at pH 8.0 and 8.5 in the absence and presence of D-glucose. Although the overall process is irreversible, according to the reheating criterion, two-dimensional deconvolution based on equilibrium thermodynamics is able to fit well the experimental DSC profiles. Such analysis gives estimates of the association constant and binding enthalpy that are in satisfactory agreement with values in the literature. The binding of D-glucose is entirely entropy-driven, since the binding enthalpy is zero. This experimental finding is rationalized by a thermodynamic cycle for the molecular association of two bodies in an aqueous solution.

REFERENCES

1. Quiocho, F.A. (1986) Carbohydrate-binding proteins: tertiary structures and protein-sugar interactions. *Annu. Rev. Biochem.* **55**, 287-315
2. Schwarz, F.P. (1988) Interaction of cytidine 3′ monophosphate and uridine 3′ monophosphate with ribonuclease A at the denaturation temperature. *Biochemistry* **27**, 8429-8436
3. Brandts, J.F. and Lin, L.N. (1990) Study of strong to ultratight protein interactions using differential scanning calorimetry. *Biochemistry* **29**, 6927-6940
4. Takeda, Y., Ross, P.D., and Mudd, C.P. (1992) Thermodynamics of Cro protein-DNA interactions. *Proc. Natl. Acad. Sci. USA* **89**, 8180-8184
5. Lin, L.N., Mason, A.B., Woodworth, R.C., and Brandts, J.F. (1994) Calorimetric studies of serum transferrin and ovotransferrin. Estimates of domain interactions, and study of the kinetic complexities of ferric ion binding. *Biochemistry* **33**, 1881-1888
6. Martinez, J.C., Filimonov, V.V., Mateo, P.L., Schreiber, G., and Fersht, A.R. (1995). A calorimetric study of the thermal stability of barstar and its interaction with barnase. *Biochemistry* **34**, 5224-5233
7. Barone, G., Catanzano, F., Del Vecchio, P., Giancola, C., and Graziano, G. (1995) Differential scanning calorimetry as a tool to study protein-ligand interactions. *Pure Appl. Chem.* **67**, 1867-1872
8. Catanzano, F., Giancola, C., Graziano, G., and Barone, G. (1996) Temperature-induced denaturation of ribonuclease S: a thermodynamic study. *Biochemistry* **35**, 13378-13385
9. Graziano, G., Catanzano, F., Giancola, C., and Barone, G. (1996) A DSC study of the thermal stability of S-protein and S-peptide/S-protein complexes. *Biochemistry* **35**, 13386-13392
10. Anderson, C.M., McDonald, R.C., and Steitz, T.A. (1978) Sequencing a protein by X-ray crystallography I. Interpretation of yeast hexokinase B at 2.5 Å resolution by model building. *J. Mol. Biol.* **123**, 1-13
11. Anderson, C.M., Stenkamp, R.E., and Steitz, T.A. (1978). Sequencing a protein by X-ray crystallography II. Refinement of yeast hexokinase B co-ordinates and sequence at 2.1 Å resolution. *J. Mol. Biol.* **123**, 15-33
12. Bennett, W. and Steitz, T.A. (1978) Glucose-induced conformational change in yeast hexokinase. *Proc. Natl. Acad. Sci. USA* **75**, 4848-4852
13. McDonald, R., Steitz, T.A., and Engelman, D. (1979) Yeast hexokinase in solution exhibits a large conformational change upon binding glucose or glucose 6-phosphate. *Biochemistry* **18**, 338-342

14. Koshland, D.E. (1963) Correlation of structure and function in enzyme action. *Science* **142**, 1533-1541
15. Straume, M. and Freire, E. (1992) Two-dimensional differential scanning calorimetry: simultaneous resolution of intrinsic protein structural energetics and ligand binding interactions by global linkage analysis. *Anal. Biochem.* **203**, 259-268
16. Straume, M. (1994) Analysis of two-dimensional differential scanning calorimetry data. Elucidation of complex biomolecular energetics. *Methods Enzymol.* **240**, 530-568
17. Takahashi, K., Casey, J., and Sturtevant, J.M. (1981). Thermodynamics of the binding of D-glucose to yeast hexokinase. *Biochemistry* **20**, 4693-4697
18. Kaji, A., Trayser, K.A., and Colowick, S.P. (1961) Multiple forms of yeast hexokinase. *Ann. N.Y. Acad. Sci.* **94**, 798-811
19. Schulze, I.T. and Colowick, S.P. (1969) The modification of yeast hexokinase by proteases and its relationship to the dissociation of hexokinase into subunits. *J. Biol. Chem.* **244**, 2306-2316
20. Schmidt, J.J. and Colowick, S.P. (1973) Chemistry and subunit structure of yeast hexokinase isoenzymes. *Arch. Biochem. Biophys.* **158**, 458-470
21. Schmidt, J.J. and Colowick, S.P. (1973) Identification of a peptide sequence involved in association of subunits of yeast hexokinases. *Arch. Biochem. Biophys.* **158**, 471-477
22. Izatt, R.M. and Christensen, J.J. (1976). Heats of proton ionization, pK, and related thermodynamic quantities in *The CRC Handbook of Biochemistry and Molecular Biology, Physical and Chemical Data* (Fasman, G.D., ed.) 3rd ed., Vol. I, pp. 151-269, CRC Press, Boca Raton, FL
23. Barone, G., Del Vecchio, P., Fessas, D., Giancola, C., and Graziano, G. (1992) Theseus: a new software package for the handling and analysis of thermal denaturation data of biological macromolecules. *J. Thermal Anal.* **38**, 2779-2790
24. Barone, G., Del Vecchio, P., Giancola, C., Graziano, G., and Riccio, A. (1994) Ligand-induced biphasic thermal denaturation of RNase A. *J. Thermal Anal.* **41**, 1263-1276
25. Freire, E. and Biltonen, R.L. (1978) Statistical mechanical deconvolution of thermal transitions in macromolecules I. Theory and application to homogeneous systems. *Biopolymers* **17**, 463-479
26. Freire, E. (1994) Statistical thermodynamic analysis of differential scanning calorimetry data: structural deconvolution of heat capacity function of proteins. *Methods Enzymol.* **240**, 502-530
27. Haynie, D.T. and Freire, E. (1994) Estimation of the folding/unfolding energetics of marginally stable proteins using differential scanning calorimetry. *Anal. Biochem.* **216**, 33-41
28. Privalov, P.L. (1979) Stability of proteins. Small globular proteins. *Adv. Protein Chem.* **33**, 167-239
29. Robert, C.H., Colosimo, A., and Gill, S.J. (1989) Allosteric formulation of thermal transitions in macromolecules, including effects of ligand binding and oligomerization. *Biopolymers* **28**, 1705-1729
30. Filimonov, V.V., Potekhin, S.A., Matveev, S.V., and Privalov, P.L. (1982) Thermodynamic analysis of scanning microcalorimetric data. Algorithms for deconvolution of complex heat absorption curves. *Mol. Biol. (USSR)* **16**, 551-562
31. Privalov, P.L. and Potekhin, S.A. (1986) Scanning microcalorimetry in studying temperature-induced changes in proteins. *Methods Enzymol.* **131**, 4-51
32. Marquardt, D. (1963) An algorithm for least-squares estimation of non-linear parameters. *J. Appl. Math.* **11**, 431-441
33. Johnson , M.L. and Frasier, G.L. (1985) Non linear least squares analysis. *Methods Enzymol.* **117**, 301-342
34. Johnson, M.L. (1992) Why, when and how biochemists should use least squares. *Anal. Biochem.* **206**, 215-225
35. Hoggett, J.G. and Kellett, G.L. (1976) Yeast hexokinase: substrate-induced association-dissociation reactions in the binding of glucose to hexokinase P-II. *Eur. J. Biochem.* **66**, 65-77
36. Kern, G., Schulke, N., Schmid, F.X., and Jaenicke, R. (1992) Stability, quaternary structure, and folding of internal, external, and core-glycosylated invertase from yeast. *Protein Sci.* **1**, 120-131
37. Barone, G., Del Vecchio, P., Giancola, C., and Graziano, G. (1995) The liquid amide transfer model and the unfolding thermodynamics of small globular proteins. *Int. J. Biol. Macromol.* **17**, 251-257
38. Graziano, G., Catanzano, F., Del Vecchio, P., Giancola, C., and Barone, G. (1996) Thermodynamic stability of globular proteins: a reliable model from small molecule studies. *Gazz. Chim. It.* **126**, 559-567
39. Sturtevant, J.M. (1941) Calorimetric investigations of organic reactions. II. A new calorimeter. The mutarotation of α and β-D-glucose. *J. Phys. Chem.* **45**, 127-147
40. Liu, Y. and Sturtevant, J.M. (1996) The observed change in heat capacity accompanying the thermal unfolding of proteins depends on the composition of the solution and on the method employed to change the temperature of unfolding. *Biochemistry* **35**, 3059-3062
41. Zale, S.E. and Klibanov, A.M. (1986) Why does ribonuclease irreversibly inactivated at high temperatures? *Biochemistry* **25**, 5432-5444
42. D'Auria, S., Rossi, M., Barone, G., Catanzano, F., Del Vecchio, P., Graziano, G., and Nucci R. (1996) Temperature-induced denaturation of β-glycosidase from the Archeon *Sulfolobus solfataricus*. *J. Biochem.* **120**, 292-300
43. Tiktopulo, E.I., Privalov, P.L., Borisenko, S.N., and Troitskii, G.V. (1985) Microcalorimetric study of domain organization of serum albumin. *Mol. Biol. (USSR)* **19**, 1072-1078
44. Edge, V., Allewell, N.M., and Sturtevant, J.M. (1985) High-resolution differential scanning calorimetric analysis of the subunits of *Escherichia coli* aspartate transcarbomoylase. *Biochemistry* **24**, 5899-5906
45. Edge, V., Allewell, N.M., and Sturtevant, J.M. (1988) Differential scanning calorimetric study of the thermal denaturation of aspartate transcarbomoylase of *Escherichia coli*. *Biochemistry* **27**, 8081-8087
46. Ross, P.D. and Shrake, A. (1988) Decrease in stability of human albumin with an increase in protein concentration. *J. Biol. Chem.* **263**, 11196-11202
47. Brandts, J.F., Hu, C.Q., Lin, L.N., and Mas, M.T. (1989) A simple model for proteins with interacting domains. Applications to scanning calorimetry data. *Biochemistry* **28**, 8588-8586
48. Lee, J.C. and Timasheff, S.N. (1981) The stabilization of proteins by sucrose. *J. Biol. Chem.* **256**, 7193-7201
49. Arakawa, T. and Timasheff, S.N. (1982). Stabilization of protein structure by sugars. *Biochemistry* **21**, 6536-6544
50. Barone, G., Catanzano, F., Del Vecchio, P., Giancola, C., and Graziano, G. (1995) Effect of D-glucose on yeast hexokinase denaturation in *Proceedings of 26èmes Journées de Calorimètrie et d'Analyse Thermique A.F.C.A.T.*, pp. 162-167, Marsiglia
51. White, T.K., Kim, J.Y., and Wilson, J.E. (1990) Differential scanning calorimetric study of rat brain hexokinase: domain structure and stability. *Arch. Biochem. Biophys.* **276**, 510-517
52. Woolfitt, A.R., Kellett, G.L., and Hoggett, J.G. (1988) The binding of glucose and nucleotides to hexokinase from *Saccharomyces cerevisiae*. *Biochim. Biophys. Acta* **952**, 238-243
53. Mayes, E.L., Hoggett, J.G., and Kellett, G.L. (1982) The binding of glucose to yeast hexokinase monomers is independent of ionic strength. *Biochem. J.* **203**, 523-525
54. Jackson, R.M. and Sternberg, M.J.E. (1995) A continuum model for protein-protein interactions: application to the docking problem. *J. Mol. Biol.* **250**, 258-275
55. Vajda, S., Weng, Z., Rosenfeld, R., and DeLisi, C. (1994) Effects of conformational flexibility and solvation on receptor-ligand binding free energies. *Biochemistry* **33**, 13977-13987
56. Weng, Z., Vajda, S., and DeLisi, C. (1996) Prediction of protein complexes using empirical free energy functions. *Protein Sci.* **5**, 614-626
57. Lee, B.K. (1985) The physical origin of the low solubility of nonpolar solutes in water. *Biopolymers* **24**, 813-823
58. Lee, B.K. (1985) A procedure for calculating thermodynamic functions of cavity formation from the pure solvent simulation data. *J. Chem. Phys.* **83**, 2421-2425
59. Lee, B.K. (1991) Solvent reorganization contribution to the transfer thermodynamics of small nonpolar molecules. *Biopoly-*

mers **31**, 993-1008
60. Finkelstein, A.V. and Janin, J. (1989) The price of lost freedom: entropy of bimolecular complex formation. *Protein Eng.* **3**, 1-3
61. Lian, Y.N., Chen, A.T., Suurkuusk, J., and Wadso, I. (1982) Polyol-water interactions as reflected by aqueous heat capacity values. *Acta Chem. Scand.* **36**, 735-739
62. Rand, R.P., Fuller, N.L., Butko, P., Francis, G., and Nicholls, P. (1993) Measured change in protein solvation with substrate binding and turnover. *Biochemistry* **32**, 5925-5929
63. Graziano, G. and Barone, G. (1996) Group additivity analysis of the heat capacity change associated with the dissolution into water of different organic compounds. *J. Am. Chem. Soc.* **118**, 1831-1835